Polymer 50 (2009) 2595–2600

Contents lists available at ScienceDirect

Polymer

journal homepage: www.elsevier.com/locate/polymer

Preparation of polymeric hybrid nanocomposites based on PE and nanosilica

Silvia Barus [a], Marco Zanetti [a,*], Massimo Lazzari [a,b], Luigi Costa [a]

[a] IFM Chemistry Department and Nanostructured Interface and Surface (NIS) Centre of Excellence, Università degli Studi di Torino, via Pietro Giuria 7, 10125 Torino, Italy
[b] Department of Physical Chemistry, Faculty of Chemistry, University of Santiago de Compostela, 15782 Santiago de Compostela, Spain

ARTICLE INFO

Article history:
Received 29 October 2008
Received in revised form
17 March 2009
Accepted 6 April 2009
Available online 16 April 2009

Keywords:
Polyethylene (PE)
Nanoscopic silica
Hybrid nanocomposite

ABSTRACT

In this study the realization of nanocomposites based on a melt dispersion of nanoscopic silica particles in a polyethylene matrix is described. Different silane coupling agents were used to improve the interaction between nanosilica and polyethylene and then to improve the dispersion of the filler. In one case vinyl groups-containing silane coupling agents containing were used. The nanocomposite obtained with this modifier was transformed in a crosslinked organic–inorganic hybrid after an electron beam radiation treatment. The nanocomposites and the hybrid were characterized with TEM and FTIR. The thermal decomposition was studied in TGA. Mechanical properties were also detected, in a small punch test and wear resistance in a rotative drum abrader.

1. Introduction

The commercial importance of polymers has been driving intense applications in the form of composites in various fields, such as aerospace, automotive, marine, infrastructure, military, etc. In recent years, composites of inorganic nanoparticles and polymers have received increasing research interests because the filler/matrix interface might constitute a much greater area of investigation and hence influence the composites' properties. The nature of the interface has been used to grossly divide these materials into two distinct classes [1]. In class I, only weak bonds (hydrogen, van der Waals or π–π bonds) between matrix and filler are present. In class II materials, the two phases are linked together through strong chemical bonds (covalent or ionic bonds). When covalent bonds are present between an organic polymer matrix and an inorganic filler we speak about hybrid materials. Nanofillers, also at low concentrations, give nanocomposites an improvement of relevant properties such as increased modulus and strength, transparency, decreased gas permeability, increased scratch, abrasion, solvent and heat resistance and decreased flammability [2]. One of the most promising properties is flame retardant. In nanocomposites based on organoclays, the lower flammability was explained in terms of ablative behaviour: when exposed to heat, the polymer matrix thermally degrade leading to the formation of a protective surface layer consisting of a filler stacking with insulating properties regarding the action of heat, oxygen and the leak of volatile products as proved by Gilman et al. [3]. Recent developments on the understanding of this mechanism have been reviewed in [4]. In some cases the effectiveness of this protective shield seems to be related to the ability of the nanofiller to enhance the formation of char between the filler particles, even in non-charring polymer. On the other hand this effect is negligible when fillers are not dispersed at the nanoscale level, indicating that the mechanism of flame retardant depends not only from the nature of the filler but also from the degree of dispersion [5]. In fibrous or particle-reinforced polymer nanocomposites, dispersion of the nanoparticle and adhesion at the particle–matrix interface play crucial roles also in determining the mechanical properties [6,7]. Increasing the adhesion between polymer and filler is needed to achieve a good dispersion. Indeed, without proper dispersion, the material will not offer improved mechanical properties over those of conventional composites, in fact, a poorly dispersed nanomaterial may reduce the mechanical properties. Additionally, by optimizing the interfacial bond between the particles and the matrix, the properties of the overall composite may be tailored improving for example properties such as interlaminar shear strength, delamination resistance, fatigue, and corrosion resistance. For example, Ou et al. have found dramatic improvements in the tensile stress (13%), strain-to-failure (138%), Young's modulus (17%) and impact strength (78%) with only 5 wt% silica nanoparticles addition to PA6 [8]. Furthermore, nanoparticles are also preferred when transparency and surface smoothness are the priorities. PMMA–silica nanocomposites showed no reduction in transparency even reinforced at relatively high loadings unlike the micrometer-sized filled systems [9,10].

* Corresponding author. Tel.: +39 011 670 7554; fax: +39 011 670 7855.
E-mail address: marco.zanetti@unito.it (M. Zanetti).

0032-3861/$ – see front matter © 2009 Elsevier Ltd. All rights reserved.
doi:10.1016/j.polymer.2009.04.012

By exploring the role of interfacial bonding in improving the performances of nanocomposites, this paper focuses on how the compatibilization between filler and matrix affect thermal or mechanical properties of nanosilica-filled polyethylene composites. In order to generate different interfacial interactions, the nanosilica particles were treated by chemical grafting with various silane coupling agents (SCAs). As a result, the following effects are expected: (i) hydrophobicity of the nanoparticles is increased, facilitating filler/matrix miscibility and a more uniform dispersion of the nanoparticles; (ii) the interfacial characteristics between the treated nanoparticles and the polymer matrix can be tailored by changing the species of the coupling agents. Dispersive mixing, which is widely used in the plastics industry, acted as the main compounding technique for preparing nanocomposites. Two different classes of silane coupling agents have been used: the network modifiers, which are molecules provided with non-reactive groups (in our case we have used silanes with an alkyl chain of different lengths) that act modifying hydrophobicity, and the network formers which are able to react with the polymer chains leading to the formation of a crosslinked network. In our case, vinyl groups-containing SCA were chosen. The formation of chemical bonding between matrix and filler through a free radical reaction has been promoted by high energy radiations that create radicals onto polymer chains, which are able to react easily and rapidly with vinyl double bonds introduced by silylation onto silica surface.

The so formed composites were characterized by FTIR and TEM to identify the dispersion and the morphology of the obtained material. Thermal properties were investigated by thermogravimetric analyses (TGAs), while mechanical properties were tested with small punch test (SPT) and abrasion test (AT).

2. Experimental

2.1. Materials

HDPE Polymer (Eraclene ML-70 type, melt flow index 2.8 g/10 min), produced by Polimeri Europa, was used as matrix for this work. The silica used to prepare nanocomposites was Silicon Dioxide Nanoparticles (SDN), Sigma–Aldrich, in the form of spherical particles of 15–20 nm diameter and density of 2.2 g/cm^3, with a specific area of 140–180 m^2/g. Vinyltriethoxysilane (VTES), hexadecyltrimethoxysilane (HDTMS) and propyltrimethoxysilane (PTMS), shipped by Sigma–Aldrich, were used as received as silane coupling agents.

2.2. Silylation of silica surface

The grafting onto silica surface of silane coupling agents was carried out by sol–gel process [11]. Before being mixed with SCA, nanoparticles were preheated at 100 °C under vacuum overnight to eliminate possible absorbed water on the surface. To 10 g nano-sized filler, intensively stirred in boiling acetone, first 5 g coupling agents and then 0.15 g maleic anhydride (MA) and 0.0225 ml of water, were added. MA has been used as acid catalyst for silylation reaction. The mixture, after the reaction time, was firstly washed several time with acetone and then refluxed for 24 h under air and then oven-dried under vacuum overnight to volatilize all unattached silane from the surface. For the convenience of this discussion, the grafted nanoparticles are denoted by: SDN–VTES, SDN–PTMS and SDN–HDTMS.

The absence of unreacted silane and silylation coverage were determined by thermogravimetric analysis (TGA) (Hi-Res TGA 2950 balance, TA Inc., with alumina pan in a 100 cm^3/min nitrogen flow and with a 10 °C/min heating ramp from room temperature up to 800 °C) on modified silica nanoparticles (Fig. 1). Silylation coverage (n_s) was calculated [12] as

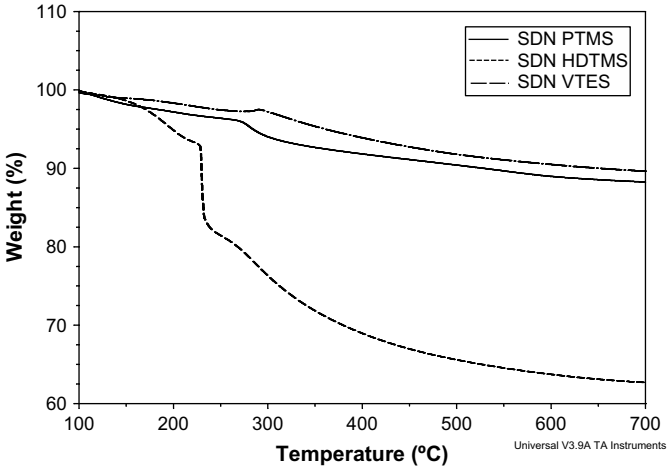

Fig. 1. TGA traces of different modified silica nanoparticles registered in oxidant atmosphere.

$$n_S = 10^6 \frac{\Delta m_s}{m_s S_s MW_{silane}}$$

wherein n_s is the silylation coverage (μmol/m^2), Δm_s is silylation weight gain for the support (g) and measured in TGA, m_s is the mass of the support material (g), S_s is the specific surface area of the support (m^2/g), and MW_{silane} is the molecular weight of the bonded silane molecule (g/mol). It is important to note that, as a silane unit hydrolyzes and/or condenses, the effective molecular weight associated with silane units will decrease. The average molecular weight, for example, for each VTES unit can theoretically be as high as 145 g/mol for the case of monolayer coverage and as low as 55 g/mol for the case of complete hydrolysis and condensation in a vinyltrialkoxysilane network. For reporting simplicity, silylation coverage in this work was calculated by using the molecular weight resulting from monodentate attachment (i.e., one bond with the surface per silane unit: 145 g/mol for VTES, 143 g/mol for PTMS and 325 g/mol for HDTMS) with no hydrolysis or condensation of the remaining ethoxy/methoxy groups. This leads to a lower limit estimate of the number of hanging groups. The calculus had to consider also weight loss of silica only in the considered temperature range, which is in our case 4.00 wt%. Silylation coverage for SDN–VTES is about 2.99 μmol/m^2, for SDN–PTMS is about 3.65 μmol/m^2 and for SDN–HDTMS 9.70 μmol/m^2.

Grafting was verified with ATR (Universal ATR Sampling Accessory assembled in a Perkin–Elmer Spectrum 100 Fourier transform infrared spectroscope, equipped with a DTGS detector) spectra. Fig. 2 shows the infrared spectra of SiO_2 as received and modified SiO_2. The collected spectra show the characteristic absorption band of modifiers, in particular, for VTES, the stretch at 1410 cm^{-1} and the in plane deformation at 1600 cm^{-1} of C=C bond and, for PTMS and HDTMS, the stretches at 2960, 2930, 2875, 2855 cm^{-1} or the deformations at 1464, 1410, 1378 cm^{-1} of $-CH_3$ and $-CH_2$ or, for HDTMS only, the rocking of $(-CH_2)_n$, $n \geq 4$, at 721 cm^{-1}. Unattached silanes vaporize from surface at oven-drying condition, than the presence of these peaks after oven treatment indicates the bonding of silane on silica surface.

2.3. Preparation and characterization of nanocomposites

The nanoparticles were melt-mixed with HDPE at a content of about 5 wt% using a Brabender internal mixer AEV330. The

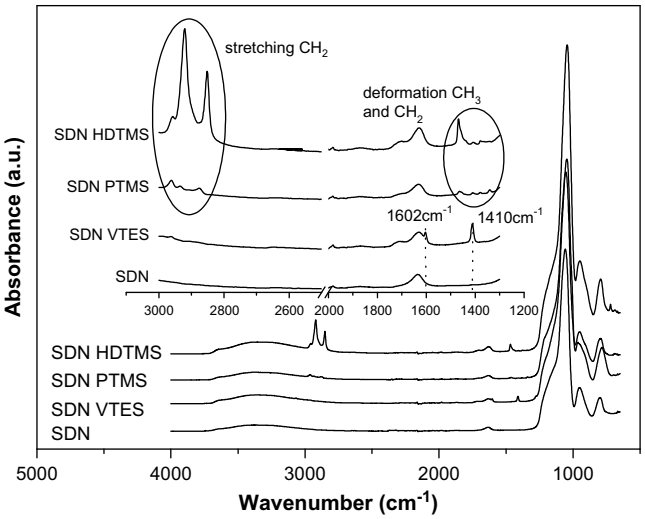

Fig. 2. FTIR spectra of SDN and modified SDN nanoparticles. In the zoomed area has been pointed out the appearance, after silylation, of the characteristic absorbances of coupling agents.

manufacturing temperature was kept at 160 °C and the screw speed amounted to 60 rpm for 10 min. After that the blends were compression-moulded into sheet samples ($50 \times 50 \times 10$ mm) at 180 ± 5 °C and 100 bar for 5 min in an industrial press. Compounds of PE and PE-unmodified silica were prepared in the same conditions to be used as references. Finally, for samples containing SDE–VTES, the formation of chemical bonding between matrix and filler has been induced by e-beam. The e-beam irradiation, with doses of 50 and 150 kGy, was performed in nitrogen atmosphere, with a 10 MeV accelerator (Bioster, Seriate, Italy), operating at 25 kW power, with a dose rate of 6×10^4 kGy/h, at room temperature. Irradiated samples are named HDPE–SDN–VTES-50 when irradiated with 50 kGy and HDPE–SDN–VTES-150 when irradiated with 150 kGy.

The distribution of silica particles in composites was studied recording images on a Philips CM-12 TEM (accelerating voltage of 120 kV) on thin sections (100 nm) cut from epoxy resin embedded samples. No staining was performed on the microtomed sections placed onto carbon-coated copper grids.

FTIR spectra of irradiated composites were recorded on a microscope FTIR Perkin–Elmer AutoIMAGE 2000 equipped with an MCT detector. Thin films, of about 150 μm, were obtained by microtoming specimens (Polycut microtome, Reichert-Jung). In a typical experiment, 16 scans were accumulated in transmission mode at 4 cm^{-1} resolution. The peak at 2020 cm^{-1}, a combination band, was used as an internal standard, since it can be regarded as unaffected by minor changes in the polymer structure. At the peak at 2020 cm^{-1}, all the spectra were normalised at an absorption of 0.05, correlating to a film thickness of ca. 100 μm.

Thermal degradation was measured on approx. 10 mg sample in an Hi-Res TGA 2950 balance, TA Inc., with alumina pan in a 100 cm^3/min air or nitrogen flow and with a 10 °C/min heating ramp from room temperature up to 800 °C.

Mechanical properties were tested with SPT performed with a hemispherical head punch, constructed following ASTM F 2183 SP standard, set in an Adamel Lhomargy DY22 machine, with a cross-head speed of 1 mm/min at room temperature. Round disk shaped specimen of 6.4 mm diameter was punched out from films with a thickness of 508 ± 5 μm, according to the standard. Experiments were carried out in triplicate. The results were plotted in terms of load [N] vs. displacement [mm]. Different samples were compared on the value of work-to-failure which is the area under the obtained curve.

Abrasion test was performed with a rotating drum abrader (Giuliani, Italy) according to UNI 9185 norm. Cylinder dimensions are 15 cm diameter and 50 cm length; above it was fixed an abrasive cloth with known roughness of 10 μm. Cylinder rotates on its own axis at an average speed of 40 turn/min for 84 turns, corresponding to 40 m. The value used to compare samples is the weight loss in g/40 m.

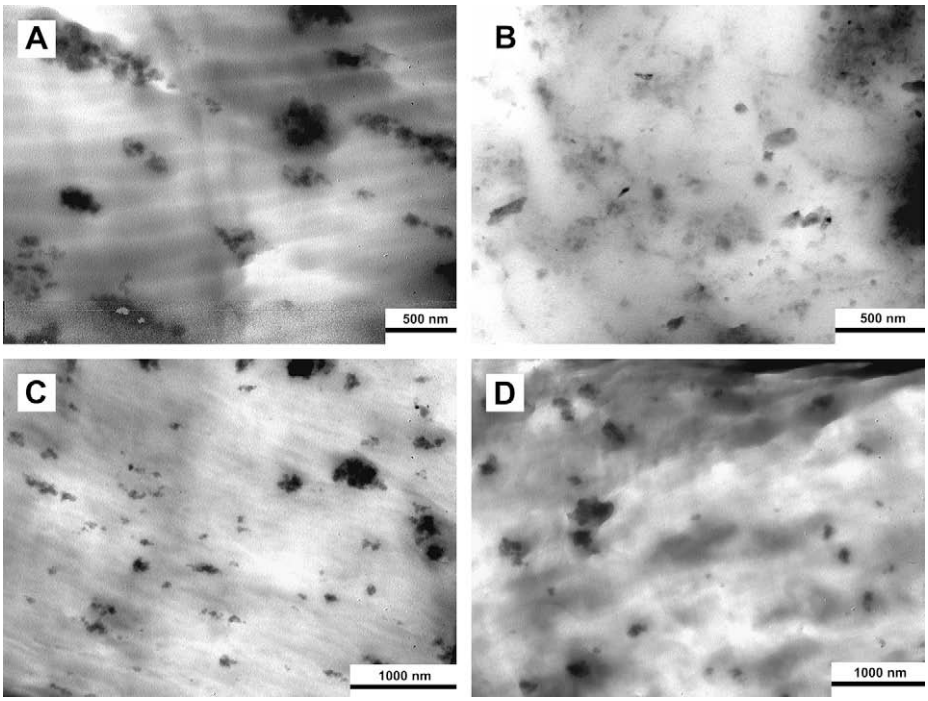

Fig. 3. TEM images of a) HDPE–SDN, b) HDPE–SDN–VTES, c) HDPE–SDN–PTMS and d) HDPE–SDN–HDTMS nanocomposites.

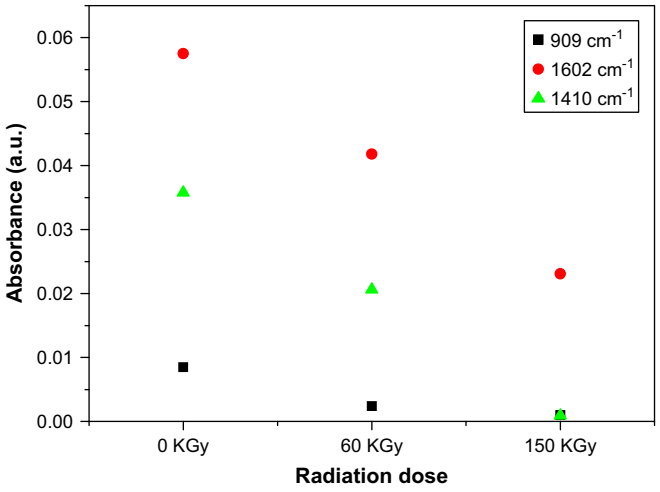

Fig. 4. Absorbance trends of C–C double bonds present in HDPE nanocomposites filled with 5 wt% of SDN–VTES: effect of radiations treatment on hybrid formation.

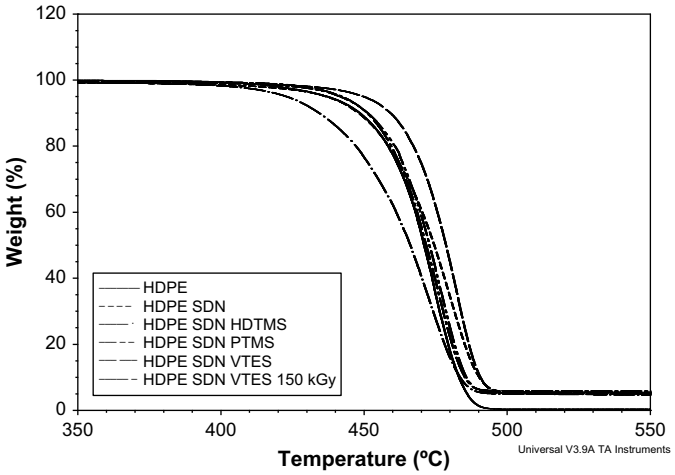

Fig. 5. TGA curves of HDPE nanocomposites filled with 5 wt% of different modified SDN nanoparticles in nitrogen atmosphere.

3. Result and discussion

3.1. Morphology of nanocomposites

TEM images are shown in Fig. 3. The dark domains represent SiO_2 particles. TEM images of all samples show a level of dispersion typical of nanocomposites. In Fig. 3a the HDPE–SDN morphology is visible; this sample shows silica aggregates whose dimensions are about 500 nm or less. Instead, in samples containing coupling agents (Fig. 3b, c and d), smaller aggregates with diameter of about 100–200 nm are visible. This phenomenon is explicable by the presence of silane coupling agents which act promoting a better dispersion of silica particles improving the miscibility between organic and inorganic phases. As expected, images of irradiated samples (not reported here) do not show differences compared to not irradiated ones.

Samples containing the network former agent were subjected to radiation treatment inducing the formation of radical species onto polymer chains. Those radicals react easily with vinyl groups of the SCA promoting the crosslink between matrix and filler. The becoming of this reaction is confirmed by the diminishing, in FTIR spectra, of the vinyl absorption band after irradiation. In Fig. 4 the absorbance of the C=C bonds (stretch at 1602 cm^{-1} and in plane deformation at 1410 cm^{-1}) vs. the radiation dose of polymer nanocomposites containing SDN–VTES is reported confirming the formation of a crosslinked hybrid material. In Fig. 4 the absorbances of vinyl group present onto polymer chains as terminals (909 cm^{-1}, vinyl CH bending) are also reported [13]. As we can see, increasing the irradiation doses all vinyl species present in samples decrease participating to the crosslink process.

3.2. Thermal properties

In polymer combustion the fuel feeding of the flame is provided by the thermal degradation of the polymer. As a consequence, the effects of the nanodispersed silica on thermal degradation of the polymer will affect the combustion process. During polymer burning, gas phase oxygen is mostly consumed by gas phase oxidation reactions (flame) and a remainder of a small amount of oxygen cannot reach the degrading sample surface against the flow of thermal degradation products evolving from the surface. Thus the study of the thermal degradation carried out under inert atmosphere (i.e. nitrogen flow) will be representative of the condensed phase mechanism during polymer combustion phenomena. Therefore TGA experiments in nitrogen are appropriate to study this mechanism. However it has been reported in literature that some nanocomposites show a strong flame retardant behaviour in cone calorimeter experiments even in absence of appreciable increasing of stability during TGA in nitrogen. On the other hand TGA under oxidant atmosphere demonstrated to be able to discriminate between nanocomposites and conventional composites showing a strong stabilization phenomena in nanocomposites as cone calorimeter experiment did. In this paper we reported TGA results both in air and in nitrogen.

Fig. 5 shows TGA curves of HDPE composites in nitrogen atmosphere. HDPE starts to lose weight at about 400 °C and at 490 °C it is completely volatilized in one step of weight loss. HDPE–SDN shows a similar behaviour in the first phase of weight loss (till 470 °C). Subsequently it shows an increasing stability until completely volatilization of polymer that occurs at 500 °C, leaving an amount of residue corresponding to the SiO_2 contained by the sample without the presence of a carbonaceous residue. Samples containing modified SDN show different trends depending on the modifier: HDPE–SDN–HDTMS is the less stable; HDPE–SDN–PTMS and HDPE–SDN–VTES-150 are stable as polyethylene only; while HDPE–SDN–VTES is the stablest one. The stabilization phenomena observed for HDPE–SND could be explained in terms of ablative behaviour: during the thermal degradation of the polymer the silica particles will accumulate to the surface of the molten polymer creating a sort of shield that acts as physical protection from heat for the remaining polymer and slowing down the volatilization of the polymer fragments generated by the pyrolysis. By this point of view the ability to form this shield will depend on the efficiency at which silica particles are able to reach each other to form a continuous barrier. In the case of HDPE–SND this barrier is created around 470 °C. On the other hand this barrier is not created in the case of HDPE–SDN–HDTMS, even in the presence of the nanosilica. Showing a lower stability than the polymer matrix this sample indicates a destabilization effect induced by HDTMS modifier that exposed to heat leads to thermal degradation generating free radicals that could accelerate the free radical chain scission of the polymer.

In samples containing VTES the stabilization seems to be more effective, even at the beginning of the degradation. This could be explained not only in terms of the physical barrier created by the nanosilica particles but also taking in to account the reactivity of vinyl double bond in respect to the macroradicals generated by the pyrolysis opposing the formation of volatile fragments stabilizing

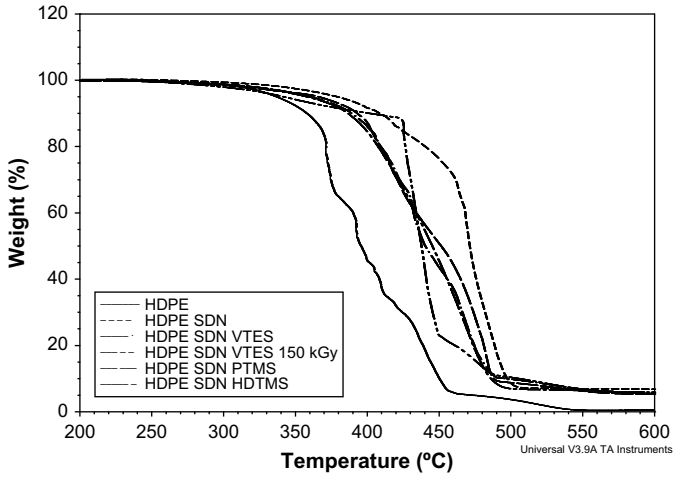

Fig. 6. TGA curves of HDPE nanocomposites filled with 5 wt% of different modified SDN nanoparticles in air atmosphere.

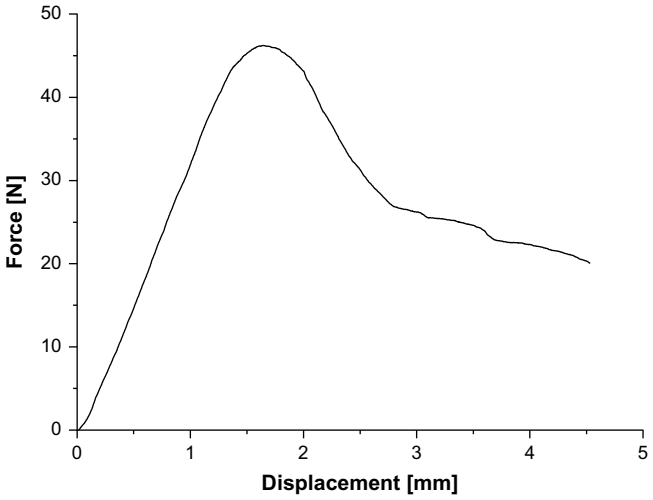

Fig. 7. Typical force–displacement curve from small punch test.

material during the first phases of thermal degradation. Moreover this mechanism increases system viscosity which some authors [14] have shown to be useful to obtain an effective flame retardancy of material.

For HDPE–SDN–VTES-150 thermal stability is lower than that of not irradiated one. The lower efficiency to create the protective barrier if compared with HDE-SDN could depend on the lower mobility of silica nanoparticles. Being covalently bonded to the polymer chain the silica nanoparticles are hampered to reach each other to create a continuous shield rendering this mechanism less efficient.

The presence of oxygen strongly decreases the stability of the PE as is evident comparing TGA curves of PE in nitrogen (Fig. 5) and air (Fig. 6). The polymer, in contact with oxygen at elevated temperatures (at about 200 °C), undergoes reactions of oxygen insertion forming peroxy radical species. The process continues with the formation of other oxidized species that, promoting chain weakening, carry out its breaking. Above 350 °C the PE is subjected, in air, to a strong weight loss to form a 10 wt% residue at 450 °C, which is completely oxidized to volatile products at 550 °C.

If compared to inert condition the silica dramatically shields polymer from the action of oxygen, increasing its thermal stability in oxidative conditions. If we consider the amount of residues at the same temperature, for example at 450 °C, we can notice that HDPE–SDN composite exhibits the highest percentage (at least 75 wt%), followed by HDPE–SDN–VTES and HDPE–SDN–PTMS with 45 wt%, SDN–HDTMS with 40 wt% and finally HDPE with 15%. SDN action is more powerful that that of modified silica. Taking in mind the morphology seen in TEM images, SDN nanocomposites present bigger agglomerate/aggregate as compared to modified SDN nanocomposites. In a mechanism involving an ablative behaviour, where the aggregation of nanoparticles is required to form an efficient shield, the nanocomposites based on SDN have a sort of pre-aggregation that could render more effective shield formation. In other words the silica aggregates have an aspect ratio rendering their behaviour in the molten polymer similar to that observed in layered silicate nanocomposites. On the other hand, the dimension of the agglomerate is away from the range of macrocomposites in which the particles are too big to be able to form the protection shield. The stabilization trend shown in Fig. 6 is inversely proportional to the dispersion degree previously observed. By this point of view it becomes clear that the presence of the silane coupling agents decreases the effect of stabilization.

For hybrid sample, HDPE–SDN–VTES-150, we can notice that the material is stable, with only 10% weight loss, up to 420 °C. At higher temperature there is a strong weight loss that brings at 450 °C at a residue of only 20%. This intermediate behaviour is due to the crosslinking which acts in two different ways: firstly, because of the network created by crosslinking of the polymer chains (both each other and with SDN particles), more C–C bonds have to be broken to produce volatile fragments, so an initial stabilization is reached; secondly, the lower mobility of SDN particle, covalently bonded to the matrix, prevents and slows down the formation of the physical shield, causing the rapidly weight loss after 420 °C.

3.3. Mechanical properties

A typical load–displacement curve from the small punch test is shown in Fig. 7. Since the loading configuration involves lateral bending, biaxial deformation, the experimental results do not directly yield the usual mechanical properties such as yield stress, elastic modulus, etc. Kurtz et al. [15] describes how they use finite element simulations to determine the elastic modulus from small punch results. Focusing on the small deformation region (the first 0.064 mm), they obtained the elastic modulus by comparing the initial slope of the experimental force–displacement curve with the corresponding slope from the finite element simulation. However, this comparison technique is quite sensitive to a number of parameters including the other mechanical properties of the specimen. Consequently, in this paper we will only report relative mechanical properties as determined by the small punch test. As a relative measure of the stiffness, we have determined the average slope of the load–displacement curve from 5 up to 35 N. The maximum load, taken as the peak force from the test result graphs, and the work-to-failure, the area under the load–displacement curve, are all shown in Fig. 8 and in Table 1. The portion of the curve used to determine the average slope includes both elastic and plastic deformation so the reported values cannot be taken as an elastic or plastic modulus. However, the values would correspond to a combination of the material resistance to deformation before and after yielding. The value of the maximum load is related to the yield strength of the material, since this point marks the transition between increasing and decreasing load during constant displacement experiments. Work-to-failure is a measure of the ability of the material to absorb energy before breaking and is related to the fracture toughness. These results clearly show that mechanical properties of HDPE are improved by the addition of nanosilica: stiffness, yield strength and fracture toughness increase with the addition of filler onto polymer matrix, improving material

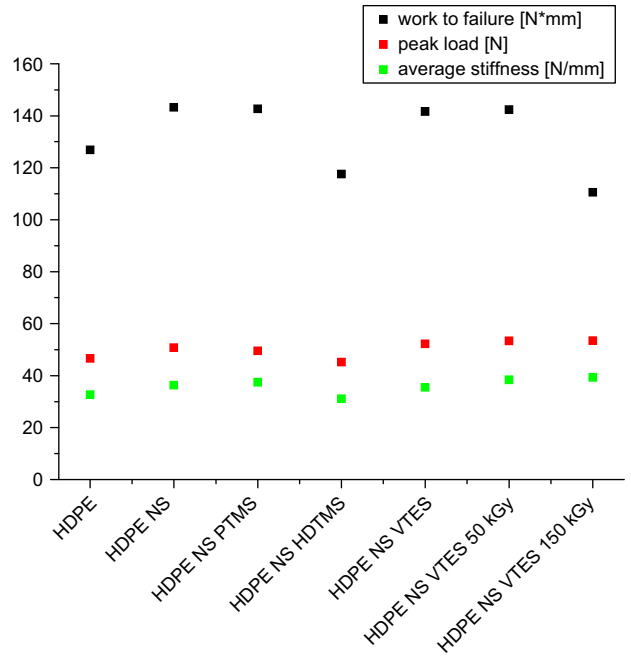

Fig. 8. Summary of mechanical properties from small punch test for samples containing different type of modified SDN and irradiated samples.

resistance. The use of modified silica did not improve mechanical properties as regard silica only. Different functionalizations lead approximately to the same result; only HDTMS decreases material properties. The use of rigid inorganic fillers as toughening agent is well recognized [16,17] and we can summarize the toughening process into three stages [18,19]: (a) stress concentration. The rigid particles act as stress concentrators owing they have different elastic properties compared to the matrix polymer and a large surface area. (b) Debonding. Stress concentration gives rise to build up of triaxial stress around the particles, leading to debonding at the particle–polymer interface. (c) Shear yielding. The voids resulting from debonding alter the stress state in the matrix polymer surrounding the voids. This reduces the sensitivity towards crazing and promotes shear yielding. Radiation treatment, for VTES samples, decreases the material toughness when radiation dose augments while the stiffness and the maximum load increase. Crosslinked samples show a reduction of elongation at break as radiation dose rises. Indeed a higher degree of crosslinking prevents the free creep of polymer chain, reducing material tenacity.

Edidin and Kurtz [20] also show that the toughness is very strongly correlated to the wear resistance of a class of polymers including polyethylene. A tenacious material, i.e. a not crosslinked one, presents a higher wear resistance as regards to reticulated ones. The results of abrasion test are reported in Table 1. Compared with the pure polymer, nanocomposites showed a lower wear resistance measured as an increase in the amount of material abraded. A better dispersion in the modified silica samples as well as the variety of modifiers used did not show noticeable differences. On the other hand the wear resistance was decreased by crosslink, showing the highest weight loss in the case of the nanocomposite irradiated at 150 kGy.

Table 1
Increase of work-to-failure, peak load and stiffness. The last column shows abrasion test result in term of weight loss.

	Radiation dose [kGy]	Work-to-failure increase [%]	Peak load increase [%]	Average stiffness increase [%]	Weight loss [g/40 m]
HDPE		0	0	0	0.0039
HDPE–SDN		13.0	8.8	11.4	0.0046
HDPE–SDN-PTMS		12.5	6.3	14.6	0.0047
HDPE–SDN–HDTMS		−7.3	−3.1	−4.9	0.0048
HDPE–SDN–VTES	0	11.7	12.1	8.7	0.0046
HDPE–SDN–VTES-50	50	12.3	14.4	17.5	0.0058
HDPE–SDN–VTES-150	150	−12.9	14.7	20.4	0.0067

4. Conclusion

Nanocomposites of HDPE were prepared by dispersing nanosilica particles with and without surface modifiers. The morphology and the degree of dispersion were observed by TEM. The functionalization of silica demonstrated to be useful to obtain a better dispersion in the organic matrix. In one case the silica surface was modified with a reactive modifier containing vinyl groups (vinyltriethoxysilane, VTES). FTIR spectra showed that crosslink reaction between the vinyl-modified nanosilica and HDPE takes place after irradiating with e-beam.

In TGA experiments the studied nanocomposites showed a stabilization phenomena similar to those reported in literature for nanocomposites based on clays. Moreover the degree of stabilization depends on the kind of surfactant employed. In nitrogen atmosphere, we have seen that the sample containing VTES results to be the most stable. In oxidant atmosphere, nanocomposites exhibits a stronger effect of stabilization compared with the pure polymer. The advantage, in term of thermal stability, is included from 50 to 100 °C. The mechanism at the basis of the effectiveness of this stabilization is dependant on the degree of filler dispersion and is facilitated when a sort of pre-aggregation is present.

Considering mechanical properties, stiffness, yield strength and fracture toughness increased in nanocomposites showing no significant differences between SDN and modified SDN. However, the wear resistance was decreased in nanocomposites.

Acknowledgements

The authors wish to thank Polimeri Europa, for polyethylene supply; BIOSTER S.p.A., Bergamo (MI), for composites irradiation and Dr. Valentina Brunella and Dr. Pierangiola Bracco, University of Turin, for helpful discussion.

References

[1] Sanchez C, Julián B, Belleville P, Popall M. J Mater Chem 2005;15:3559–92.
[2] Hussain F, Hojjati M, Okamoto M, Gorga R. J Compos Mater 2006;40(17):1511–75.
[3] Gilman JW. Appl Clay Sci 1999;15:31–49.
[4] Zanetti M. In: Mai YW, Yu ZZ, editors. Polymer nanocomposites. Cambridge: Woodhead Publishing Limited; 2006. p. 256–72.
[5] Zanetti M, Bracco P, Costa L. Polym Degrad Stab 2004;85:657–65.
[6] Fiedler B, Gojny FH, Wichmann MHG, Nolte MCM, Schulte K. Compos Sci Technol 2006;66:3115–25.
[7] Dondero WE, Gorga RE. J Polym Sci Part B Polym Phys 2006;44:864–78.
[8] Qu Y, Yang F, Yu ZZ. J Polym Sci Part B Polym Phys 1998;36:789–95.
[9] Yu YY, Chen CY, Chen WC. Polymer 2003;44:593–601.
[10] Liu YL, Hsu CY, Hsu KY. Polymer 2005;46:1851–6.
[11] Bauer F, Ernst H, Decker U, Findeisen M, Glasel H, Langguth H, et al. Macromol Chem Phys 2000;201:2654–9.
[12] Yoshida W, Castro RP, Jou JD, Cohen Y. Langmuir 2001;17:5882–8.
[13] Bracco P, Brunella V, Luda MP, Zanetti M, Costa L. Polymer 2005;46:10648–57.
[14] Kashiwagi T, Mu M, Winey K, Cipriano B, Raghavan SR, Pack S, et al. Polymer 2008;49:4358–68.
[15] Kurtz SM, Foulds JR, Jewett CW, Srivastav S, Edidin AA. Biomaterials 1997;18(24):1659–63.
[16] Kim GM, Michler GH. Polymer 1998;39:5689–98.
[17] Kim GM, Michler GH. Polymer 1998;39:5699–703.
[18] Zuiderduin CJ, Westzaan C, Huetink J, Gaymans RJ. Polymer 2003;44:261–75.
[19] Terselius B, Gedde UW, Jansson JF. In: Brostow W, Corneliussen RD, editors. Failure in plastics. Monaco: Hanser Publishers; 1986 [chapter 14].
[20] Edidin AA, Kurtz SM. Funct Biomater 2001;198:1–40.